Int. J. Devl Neuroscience 40 (2015) 76–84

Contents lists available at ScienceDirect

International Journal of Developmental Neuroscience

journal homepage: www.elsevier.com/locate/ijdevneu

Development of non-catecholaminergic sympathetic neurons in para- and prevertebral ganglia of cats

Petr M. Masliukov[a,*], Andrey I. Emanuilov[a], Konstantin Moiseev[a], Alexandr D. Nozdrachev[b], Svetlana Dobrotvorskaya[c], Jean-Pierre Timmermans[d]

[a] Department of Normal Physiology, Yaroslavl State Medical Academy, Revoliucionnaya 5, Yaroslavl 150000, Russia
[b] Department of Physiology, St. Petersburg State University, St. Petersburg, Russia
[c] Kazan (Volga Region) Federal University, Kazan, Russia
[d] Laboratory of Cell Biology and Histology, Department of Veterinary Sciences, University of Antwerp, Antwerp, Belgium

ARTICLE INFO

Article history:
Received 26 November 2014
Accepted 5 December 2014
Available online 6 December 2014

Keywords:
Autonomic nervous system
Sympathetic ganglia
Cholinergic neurons
Nitric oxide
Vasoactive intestinal peptide
immunohistochemistry
Postnatal development

ABSTRACT

Expression of vasoactive intestinal peptide (VIP), neuronal nitric oxide synthase (nNOS), choline acetyltransferase (ChAT) and calcitonin gene-related peptide (CGRP) in the sympathetic ganglia was investigated by immunohistochemistry in the superior cervical ganglion (SCG), stellate ganglion (SG) and celiac ganglion (CG) from cats of different ages (newborn, 10-day-old, 20-day-old, 30-day-old and 2-month-old). Non-catecholaminergic TH-negative VIP-immunoreactive (IR) and nNOS-IR sympathetic ganglionic neurons are present from the moment of birth. In all studied age groups, substantial populations of VIP-IR (up to 9.8%) and nNOS-IR cells (up to 8.3%) was found in the SG, with a much smaller population found in the SCG (<1%) and only few cells observed in the CG. The percentage of nNOS-IR and VIP-IR neurons in the CG and SCG did not significantly change during development. The proportion of nNOS-IR and VIP-IR neuron profiles in the SG increased in first 20 days of life from 2.3 ± 0.15% to 8.3 ± 0.56% and from 0.3 ± 0.05% to 9.2 ± 0.83%, respectively. In the SG, percentages of nNOS-IR sympathetic neurons colocalizing VIP increased in the first 20 days of life. ChAT-IR and CGRP-IR neurons were not observed in the sympathetic ganglia of newborn animals and did not appear until 10 days after birth. In the SG of newborn and 10-day-old kittens, the majority of NOS-IR neurons were calbindin (CB)-IR, whereas in the SCG and CG of cats of all age groups and in the SG of 30-day-old and older kittens, the vast majority of NOS-IR neurons lacked CB. We conclude that the development of various non-catecholaminergic neurons in different sympathetic ganglia has its own time dynamics and is concluded at the end of the second month of life.

1. Introduction

The vast majority of sympathetic ganglionic neurons are catecholaminergic and contain specific synthetic enzymes including tyrosine hydroxylase (TH), aromatic amino acid decarboxylase and dopamine β hydroxylase. Some sympathetic neurons lack catecholamines and mostly use acetylcholine as their main neurotransmitter. Cholinergic sympathetic neurons are present in the stellate ganglion (SG) and other thoracic sympathetic chain ganglia, but are rare in the superior cervical ganglion (SCG) and prevertebral ganglia (Weihe et al., 1996; Schäfer et al., 1998; Anderson et al., 2006). In mammals, these neurons innervate sweat glands and the periosteum (Asmus et al., 2001). In cats and dogs, but not in rodents, monkeys or humans, cholinergic sympathetic neurons also innervate arterial blood vessels in skeletal muscle (Bolem and Fuxe, 1970; Järhult et al., 1980; Klimaschewski et al., 1996).

All cholinergic sympathetic neurons also express vasoactive intestinal peptide (VIP). In rats, sudomotor neurons contain VIP and calcitonin gene-related peptide (CGRP) and always lack calbindin D28 K (CB). Cholinergic neurons innervating the periosteum contain VIP and sometimes CB, but always lack CGRP (Anderson et al., 2006). Two subclasses of VIP-positive cells are found in cat sympathetic ganglia: scattered sympathetic ganglion neurons expressing immunoreactivity (IR) for CGRP in addition to VIP and acetylcholinesterase (AChE), and clustered VIP and AChE-positive cells lacking CGRP IR (Lindh et al., 1989).

In cats, some cholinergic postganglionic neurons also express neuronal nitric oxide synthase (nNOS), which is detected in 99% of the presumptive sudomotor neurons exhibiting CGRP and VIP IR and in 70% of the presumptive muscle vasodilator neurons containing VIP but not CGRP (Anderson et al., 1995).

* Corresponding author. Tel.: +7 0852 305763, fax: +7 0852 305013.
E-mail address: mpm@yma.ac.ru (P.M. Masliukov).

http://dx.doi.org/10.1016/j.ijdevneu.2014.12.004
0736-5748/

Current data about the development of cholinergic sympathetic ganglionic neurons are conflicting. Despite considerable insight into this critical developmental process, key features of cholinergic neuronal development are still subject to debate. It has been hypothesized that cholinergic sympathetic innervation of sweat glands in rat and mouse is the result of a postnatal switch from a fully functional noradrenergic phenotype to a cholinergic phenotype under the influence of target-derived factors, and IR for ChAT, VIP and CGRP is not detectable during the first postnatal week (Landis, 1988). On the other hand, some cholinergic sympathetic neurons are already present prenatally and hence long before target innervation, i.e., their neurochemical phenotype developed target-independent (Schäfer et al., 1997; Masliukov et al., 2006; Schütz et al., 2008). In newborn rodents, the vast majority of cholinergic sympathetic ganglionic neurons are initially noradrenergic and display IR for both ChAT and TH. TH IR disappears in the first 20 days of life (Masliukov et al., 2003). Thus, cholinergic sympathetic differentiation seems to be complex, involving either both target-independent and target-dependent control or only target-induced differentiation, according to the specific neuronal subpopulation and target (Ernsberger and Rohrer, 1999).

In rodents, nNOS-positive neurons are not present in sympathetic neurons from birth onwards. In cats, we previously found some changes in the number of sympathetic neurons expressing NADPH-d. In the SG, the proportion of NADPH-d-positive cells increased in the first 20 days and then decreased again between the first and the second month of life (Emanuilov et al., 2008). NADPH-d histochemistry is often used to label nNOS-containing neurons in the nervous system (Hope et al., 1991; Santer and Symons, 1993). However, if was found that a slight mismatch between nNOS-immunostaining and NADPH-d staining may occur and that some nNOS-positive structures can be labeled in the absence of NADPH-d (Spessert et al., 1994). In this respect,no data about the postnatal development of sympathetic ganglionic nNOS-IR neurons are available.

In kittens, many sympathetic neurons in the SG contain CB. During development, the number of CB-IR neurons rapidly decreases in the first two months of life, and only scattered CB-IR neurons are found in the sympathetic ganglia of older cats (Masliukov et al., 2012). CB is a member of the EF-hand family of calcium-binding proteins, which are involved in numerous functions, including cell signaling, calcium uptake and transport, cell motility and intracellular calcium buffering (Andressen et al., 1993; Schwaller, 2012). Obviously, CB plays an important role in the development of sympathetic neurons but the colocalization of CB with different types of neurotransmitters in the sympathetic ganglia of mammals at different stages of ontogenesis remains to be elucidated.

Taking together, the purpose of this study was to gain further insight into the neuroplasticity of sympathetic neurons during early postnatal ontogenesis by comparing the development of non-catecholaminergic neurons expressing different markers in para- and prevertebral sympathetic ganglia. In the current work, we performed our experiments on cats since NOS-IR neurons are absent in rodents (Emanuilov et al., 2008; Masliukov et al., 2014) and because the highest numbers of nitrergic neurons are observed in the cat and human sympathetic ganglia (Klimaschewski et al., 1996).

2. Experimental procedures

2.1. Animals

All animal procedures were approved by the Institutional Animal Care and Use Committee of the Yaroslavl State Medical Academy and were conducted in accordance with the "Guide for the Care and Use of Laboratory Animals" (NIH Publication No. 85–23, revised 1996) as well as the relevant Guidelines of the Russian Ministry of Health for scientific experimentation on animals.

Newborn, 10-day-old, 20-day-old, 30-day-old cats and 2-month-old (5 groups each containing 5 animals) were used in this work to study the localization and morphological parameters of ChAT-, nNOS-, VIP-, CGRP-IR neurons in sympathetic ganglia. All animals were kept in an acclimatized room (12/12 h light/dark cycle; 22 ± 3 °C) and were provided with water and pellets ad libitum.

2.2. Tissue preparation

All animals were sacrificed with a lethal dose of sodium pentobarbital (Nembutal®, 300 mg/kg, i.p.), after which they were perfused transcardially with 500 ml of physiological saline and 1 ml heparin followed by a similar volume of fixative composed of 4% paraformaldehyde (PF) in 0.1 M phosphate buffer. After perfusion, the superior cervical (SCG), stellate (SG) and celiac ganglia (CG) from each side were dissected out, rinsed in physiological solution and immersed in 4% PF for 1–2 h at room temperature. Following fixation, they were washed in three 30-min changes of phosphate-buffered saline (PBS; 0.01 M; pH 7.4), cryoprotected by overnight immersion in 20% buffered (pH 7.4) sucrose solution at 4 °C, mounted in TissueTek (Sakura Finetek Europe, the Netherlands) on a cryostat chuck and frozen. Twelve-μm-thick cross sections were cut with a cryostat, mounted on poly-L-lysine-coated slides and air-dried for 1 h.

2.3. Immunohistochemistry

Serial sections of the SCG, SG and CG were processed for immunohistochemistry. The sections were pre-incubated for 30 min at room temperature with blocking buffer containing 5% normal donkey serum (Jackson ImmunoResearch Laboratories, USA) and 0.3% Triton X-100 (Sigma, USA) in PBS to prevent non-specific binding of secondary antibodies. In order to visualize ChAT, CGRP, VIP, nNOS, TH, CB, single or double immunostaining with antibodies (raised in different host species; see Table 1a) was performed.

Subsequently, the sections were incubated in the primary antisera for 24 h at room temperature, rinsed in PBS and further incubated in the corresponding secondary antisera for 2 h at room temperature (see Table 1b). In some experiments, sections were

Table 1a
Primary antisera used for immunohistochemistry.

Primary antisera	Host species	Dilution	Source
nNOS	Goat	1:300	Abcam, ab1376
nNOS	Rabbit	1:20	LifeSpan BioSciences, LS-B8696
VIP	Rabbit	1:200	Abcam, ab43841
TH	Sheep	1:1000	Abcam, ab113
ChAT	Goat	1:50	Millipore, AB144P
CGRP	Goat	1:200	Abcam, ab36001
CB	Rabbit	1:500	Abcam, ab11426
CB	Mouse	1:300	Abcam, ab82812

Table 1b
Secondary antisera used for immunohistochemistry.

Secondary antisera	Dilution	Source
Donkey anti-goat IgG FITC	1:200	Jackson immunoresearch
Donkey anti-goat IgG CY3	1:200	Jackson immunoresearch
Donkey anti-rabbit IgG FITC	1:200	Jackson immunoresearch
Donkey anti-rabbit IgG CY3	1:200	Jackson immunoresearch
Donkey anti-mouse IgG CY3	1:200	Jackson immunoresearch
Donkey anti-sheep IgG CY3	1:200	Jackson immunoresearch

CY3 – cyanine 3, FITC – fluorescein isothiocyanate.

Table 2
Percentages of VIP-IR and nNOS-IR neurons in the cat sympathetic ganglia ($n = 5$ in each age group, each ganglion).

Age	VIP-IR		nNOS-IR	
	SCG	SG	SCG	SG
Newborn	0.1 ± 0.05	0.3 ± 0.1	0.3 ± 0.03	2.3 ± 0.2*
10-day-old	0.6 ± 0.1	5.6 ± 0.4*	0.7 ± 0.1	5.6 ± 0.3*
20-day-old	0.6 ± 0.3	9.2 ± 0.8*	0.9 ± 0.2	8.3 ± 0.6*
1-month-old	0.5 ± 0.5	9.6 ± 1.1*	0.6 ± 0.2	7.2 ± 0.4*
2-month-old	0.7 ± 0.3	9.8 ± 0.6*	0.8 ± 0.26	6.8 ± 0.3*

* $p < 0.05$, statistically significant differences between SCG.

counterstained for 20 min at room temperature with NeuroTrace red (Molecular Probes, N-21482, USA) diluted 1:200 in blocking buffer. The sections were then rinsed three final times in PBS, mounted on glass slides, allowed to dry overnight and coverslipped using VectaShield (Vector Bioproducts, USA). The control experiments were carried out with the primary antibody replaced with NDS.

2.4. Image processing and statistics

The specimens were examined using an Olympus BX43 fluorescence microscope (Tokyo, Japan) fitted with filter sets that allow separate visualisation of FITC, CY3 or NeuroTrace red. Images from the fluorescence microscope were recorded using a TCH 5.0 cooled CCD digital camera and ISCapture version 3.6 for Windows imaging software (Tucsen, China). Each image was processed using a sharpen filter and contrast and brightness adjustment only. All photomicrographic plates were made using Adobe Photoshop 7.0 software (Adobe Systems, USA). To calculate the percentage of IR neuronal profiles in the ganglia, three central longitudinal sections (i.e., where the ganglionic nerves emerge from the ganglion) were taken from each ganglion at a distance of approximately 50 μm. To avoid duplicate counts of neurons in the serial sections of the ganglia, only those nerve cell bodies containing a clearly identified nucleus were counted in any given section. To determine the percentage of ChAT-IR, VIP-IR or NOS-IR profiles, we counted the total number of labeled neurons in the measured area and considered them as 100%. IR neuronal profiles were counted in randomly selected measured areas (1 microscopic field was 0.12 mm^2) at 200-fold magnification. Data from 10 measured areas per ganglion per age group, per animal, were included in this study. Data from individual ganglia in each age group were meaned, yielding group sizes of $n = 5$. Cross-sectional areas of nNOS-IR profiles were determined using ImageJ software (http://imagej.nih.gov/ij/index.html).

Statistical methods include calculation of the mean and standard error of the mean. Differences in means were subjected to one-way ANOVA, followed by Tukey's post-test of multiple comparisons and Chi-square test. Differences were considered statistically significant if $p < 0.05$.

In the running text below and above, the binding or immunoreactivity of a marker molecule in a profile is designated with a plus sign (e.g., nNOS+); conversely, the absence of binding or immunoreactivity is indicated with a minus sign (e.g., nNOS−).

3. Results

3.1. VIP-IR and nNOS-IR neurons in sympathetic ganglia during postnatal development

VIP-IR and nNOS-IR neurons were observed in all studied sympathetic ganglia in cats from birth onwards (Fig. 1). VIP immunolabelling produced diffuse cytoplasmic speckling and a more diffuse perinuclear ring. nNOS labelling was evenly distributed throughout the cytoplasm of the cell body, filled the cytoplasm and proximal processes but appeared to be absent from the distal processes. Three populations of VIP-IR and nNOS-IR neurons were identified: VIP+/nNOS−, VIP+/nNOS+ and VIP−/nNOS+. The largest number of VIP-IR and nNOS-IR neuron profiles was located in the SG in comparison with the SCG and CG (Table 2). The lowest number of VIP-IR cell profiles in the SG was observed in newborn kittens. These neurons increased in number during the first 20 days of development (Table 2). Differences between newborn, 10-day-old and 20-day-old animals were statistically significant ($p < 0.05$).

Table 3
Percentages of VIP-IR sympathetic ganglionic neurons co-localizing nNOS ($n = 5$ in each age group, each ganglion) (%).

Age	SCG	SG
Newborn	93 ± 0.6	31 ± 4.1
10-day-old	92 ± 0.5	51 ± 3.4*
20-day-old	93 ± 0.6	54 ± 2.2*
1-month-old	93 ± 0.7	47 ± 1.8*
2-month-old	92 ± 1.0	48 ± 3.0*

* $p < 0.05$, statistically significant differences with newborns.

Two groups of VIP-IR neurons were identified in the cat sympathetic ganglia in terms of their distribution pattern: they occur either scattered or clustered. In the SG, some VIP-IR cells were clustered while other cells were diffusely distributed. VIP-IR clusters containing 3–20 neurons, were located among the bundles traversing the SG and around the origin of the nerve trunks leaving the ganglion. Clustered VIP-IR neuron profiles were intensely immunoreactive as opposed to the weakly labelled, scattered VIP-IR neurons.

In the SG of newborn kittens, VIP-IR neurons were found predominantly in clusters with a few single VIP+ cells found outside of the clusters. In the SG of 10-day-old kittens, the number of scattered VIP-IR neurons increased and in 20-day-old kittens their number was the same as in adult cats. In the SCG and CG, single VIP-IR neuron profiles were scattered throughout the ganglion.

In the SCG, the percentage of VIP-IR and nNOS-IR neuron profiles was very small without statistically significant differences between the different age groups ($p > 0.05$). The CG contained only single VIP-IR and nNOS-IR cell profiles in all age groups.

In the SG, nNOS-IR neuron profiles were scattered mainly in the lateral part of the ganglion. In newborn kittens, the number of nNOS-IR neuron profiles was still low but significantly increased in the first 20 days ($p < 0.01$). The percentage of nNOS-IR neuron profiles declined between 20 days and 2 months of age (Table 2).

In the SCG, almost all VIP-IR sympathetic ganglionic neurons co-localized nNOS and in the CG all VIP-IR neurons were also nNOS-IR.

In the SG, the percentage of VIP-IR neurons co-localizing nNOS substantially increased in the first 10 days (Table 3). Many scattered VIP-IR neuron profiles becoming also nNOS+ appeared in the SG at 20 days. In the SG, the majority of nNOS-IR neurons were VIP-negative in newborn kittens (Table 4). The percentage of nNOS-IR neurons co-localizing VIP decreased in 10-day-old kittens but increased again in 20-day-old animals.

Table 4
Percentages of nNOS-IR sympathetic ganglionic neurons co-localizing VIP ($n = 5$ in each age group, each ganglion) (%).

Age	SCG	SG
Newborn	94 ± 0.6	38 ± 1.9
10-day-old	94 ± 0.9	25 ± 1.7*
20-day-old	93 ± 0.5	68 ± 2.2*
1-month-old	94 ± 0.4	73 ± 1.8*
2-month-old	95 ± 0.6	75 ± 2.4*

* $p < 0.05$, statistically significant differences with newborns.

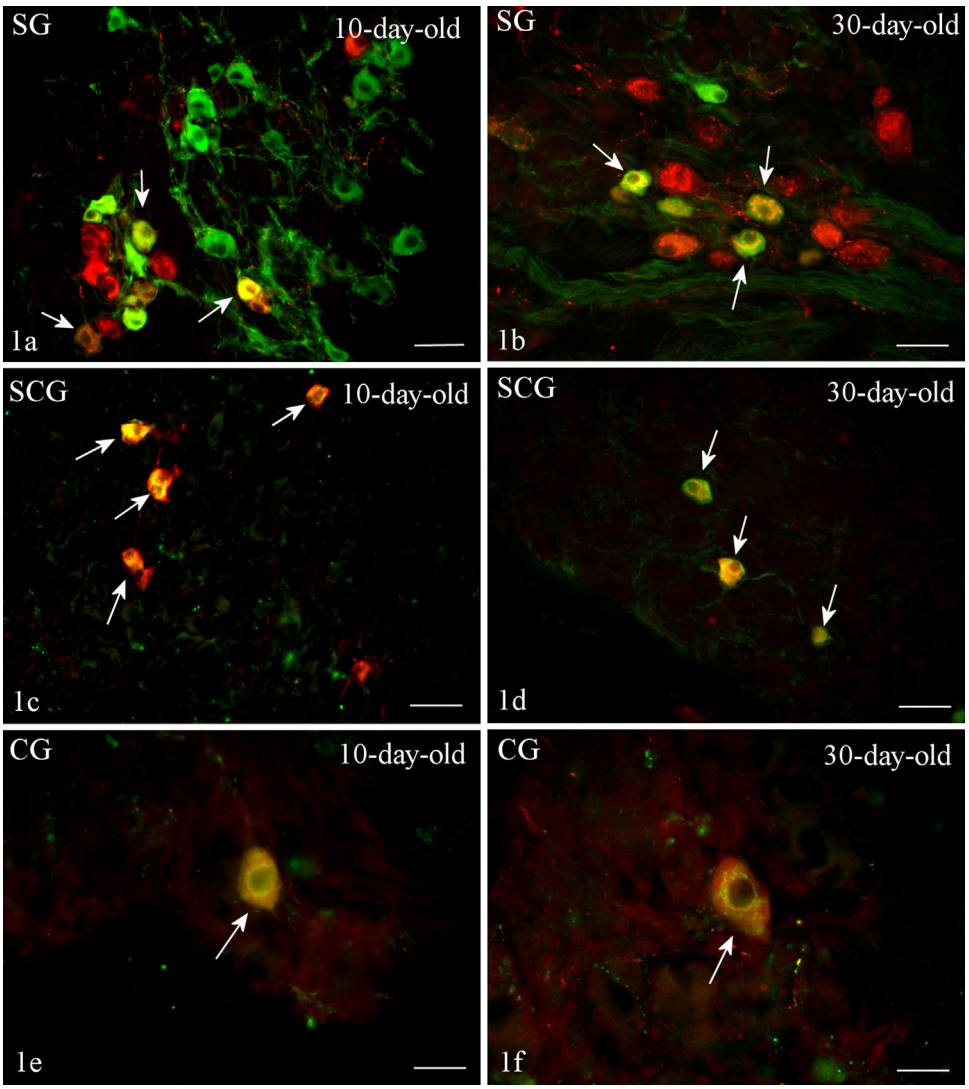

Fig. 1. Fluorescence micrographs of nNOS-IR (green) and VIP-IR (red) neurons in the SG (a and b), SCG (c and d) and CG (e and f) in 10-day-old (a, c, e) and 30-day-old cats (b, d, f). nNOS+/VIP+ IR neurons are indicated by arrows. Bar 50 μm (a–d), 25 μm (e and f). (For interpretation of the references to color in this figure legend, the reader is referred to the web version of this article.)

In the SCG, SG and CG of all studied animals, almost all nNOS-IR and VIP-IR neurons were TH-negative (Fig. 2), except for a few VIP/TH+ neurons in the SG of newborn kittens.

The mean of the cross-sectional area of VIP-IR and nNOS-IR neuron profiles increased during development in all studied sympathetic ganglia (Table 5). From the moment of birth, the mean of the cross-sectional area of VIP-IR and nNOS-IR neuron profiles was larger in comparison with TH-IR cell profiles ($p < 0.05$). We did not observe any statistically significant differences in this parameter between VIP+/nNOS−, VIP+/nNOS+ and VIP−/nNOS+ neuron profiles (Table 6, $p > 0.05$). The cross-sectional area of VIP-IR and nNOS-IR neuron profiles was larger in the SG than in the SCG.

3.2. ChAT-IR and CGRP-IR sympathetic ganglionic neurons in postnatal development

Only single ChAT-IR neuron profiles were found in newborn kittens in all studied sympathetic ganglia. After 10 days, all ChAT-IR neurons also expressed VIP and vice versa in the SCG, SG and CG (Fig. 3).

CGRP-IR neurons were found scattered throughout all studied sympathetic ganglia but did not form clusters (Fig. 4). CGRP-IR neurons were absent in newborn animals, appeared only in 10-day-old cats and also contained VIP and nNOS in the SCG and CG of 10-day-old and older animals.

In the SG of 10-day-old kittens, only 23 ± 4.2% of VIP-IR neuron profiles were CGRP-IR and 12 ± 4.0% of nNOS-IR cells were also CGRP-IR. In 20-day-old kittens, the percentage of VIP-IR neurons co-localizing CGRP increased to 44 ± 2.5% and the proportion of nNOS+/CGRP+ neuron profiles augmented to 93 ± 2.5% and did not change during further development.

3.3. Co-localization of CB with VIP and nNOS in sympathetic neurons during postnatal development

The highest number of CB-IR neuron profiles was found in newborn and 10-day-old kittens, after which CB-IR neurons rapidly decreased in number during the first two months of life (Fig. 5). Only single CB-IR neuron profiles were found in the SCG and SG of two-month-old cats and in the CG at all studied ages.

In the SCG, nNOS-IR and VIP-IR neuron profiles were largely CB-negative at all studied ages and only a few nNOS+/CB+ or VIP+/CB+ neurons were found. In the CG, all nNOS-IR and VIP-IR neurons lacked CB-IR.

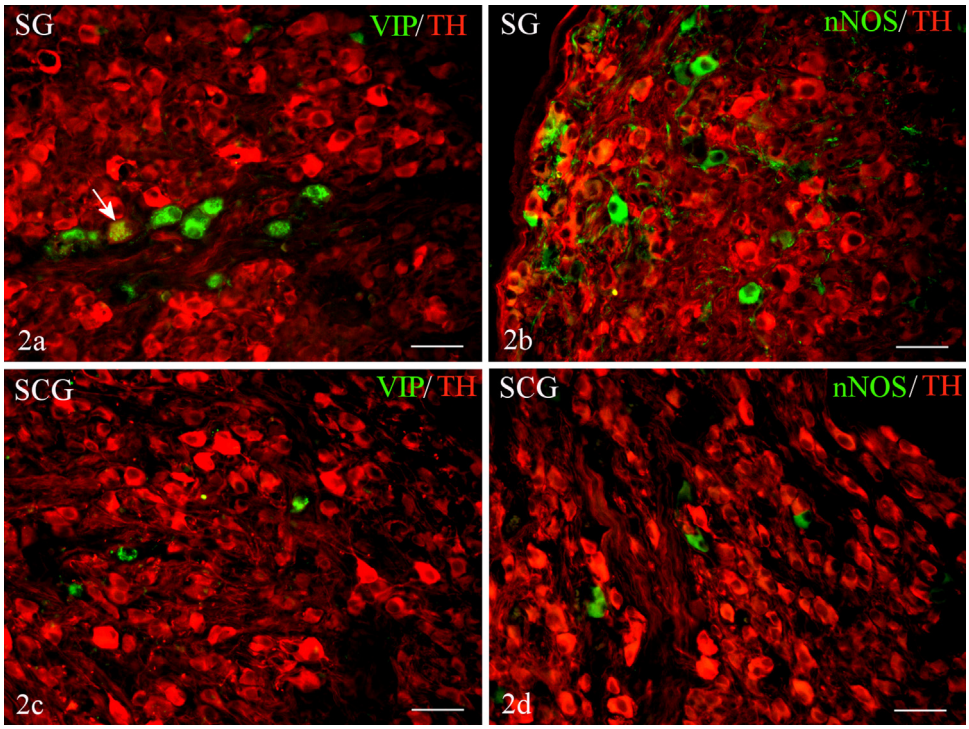

Fig. 2. Fluorescence micrographs of TH-IR (red), VIP-IR (green, a, c), nNOS-IR (green, b, d) neurons in the SG (a and b), SCG (c and d) in newborn kittens. Single co-localization of TH and VIP is indicated by arrow (a). Bar 50 μm. (For interpretation of the references to color in this figure legend, the reader is referred to the web version of this article.)

Table 5
Cross-sectional areas of nNOS-IR, VIP-IR and TH-IR neurons in the SG and SCG of cats of different ages ($n = 100$ in each age group, SG and SG; $n = 30$ in CG).

Age	SG			SCG			CG		
	nNOS	VIP	TH	nNOS	VIP	TH	nNOS	VIP	TH
Newborn	316 ± 16.4*	325 ± 19.5*	223 ± 7.8	227 ± 18.5*	232 ± 14.3*	183 ± 30.5	335 ± 43.2*	344 ± 38.5*	264 ± 12.6
10-day-old	354 ± 15.3*	338 ± 26.2*	245 ± 11.5	307 ± 22.1*	289 ± 15.6*	203 ± 30.5	398 ± 38.4*	396 ± 41.3*	289 ± 13.8
20-day-old	437 ± 21.5*	412 ± 21.6*	274 ± 18.4	339 ± 21.5*	318 ± 18.2*	223 ± 30.5	452 ± 21.5*	437 ± 38.7*	324 ± 22.1
1-month-old	512 ± 23.4*	506 ± 30.8*	346 ± 23.2	419 ± 24.8*	427 ± 21.5*	268 ± 30.5	564 ± 62.7*	552 ± 53.5*	375 ± 24.6
2-month-old	626 ± 31.9*	638 ± 23.2*	423 ± 19.6	467 ± 27.6*	472 ± 25.2*	316 ± 30.5	653 ± 52.7*	649 ± 48.3*	489 ± 42.7

* $p < 0.05$, statistically significant differences with TH-IR neurons at the same age.

Table 6
Cross-sectional areas of nNOS+/VIP- (nNOS), nNOS+/VIP+ (nNOS/VIP) and nNOS-/VIP+ (VIP) neurons in the SG and SCG of cats of different ages ($n = 100$ in each age group, each ganglion).

Age	SG			SCG	CG
	nNOS	nNOS/VIP	VIP	nNOS/VIP	nNOS/VIP
Newborn	294 ± 12.7*	318 ± 14.7*	324 ± 16.9*	243 ± 19.9	326 ± 35.6*
10-day-old	372 ± 15.3*	342 ± 24.4	350 ± 13.7	311 ± 20.3	401 ± 32.3*
20-day-old	433 ± 38.2*	404 ± 22.2	426 ± 25.6*	349 ± 26.8	468 ± 31.6*
1-month-old	501 ± 23.4*	488 ± 30.8	492 ± 27.2	435 ± 28.2	566 ± 58.2*
2-month-old	580 ± 31.9*	568 ± 23.2*	596 ± 24.9*	478 ± 30.5	644 ± 63.1*

* $p < 0.05$, statistically significant differences with neurons in SCG at the same age.

In the SG of newborn kittens, 63 ± 4.2% of nNOS-IR neuron profiles were CB-IR. In 10-day-old animals, their number decreased to 48 ± 5.2% and in 20-day-old animals, 53 ± 3.6% of the nNOS-IR neurons were CB-IR. In 30-day-old cats, their number substantially decreased to 12 ± 1.4%, and in 2-month-old cats, all nNOS-IR neurons were CB-negative.

In newborn kittens, all VIP-IR neurons in the SG were devoid of CB IR. In 10-day-old animals, the percentage of VIP+/CB+ neuron profiles was 8 ± 1.3%, in 20-day-old cats – 11 ± 1.6% and in 30-day-old cats – 2 ± 0.4%.VIP+/CB+ neurons were no longer observed in two-month-old cats.

4. Discussion

The present study reveals a number of morphological changes in VIP-IR, nNOS-IR, ChAT-IR and CGRP-IR neurons in the para- and prevertebral ganglia of cats during postnatal development. In cats, non-catecholaminergic sympathetic ganglionic neurons

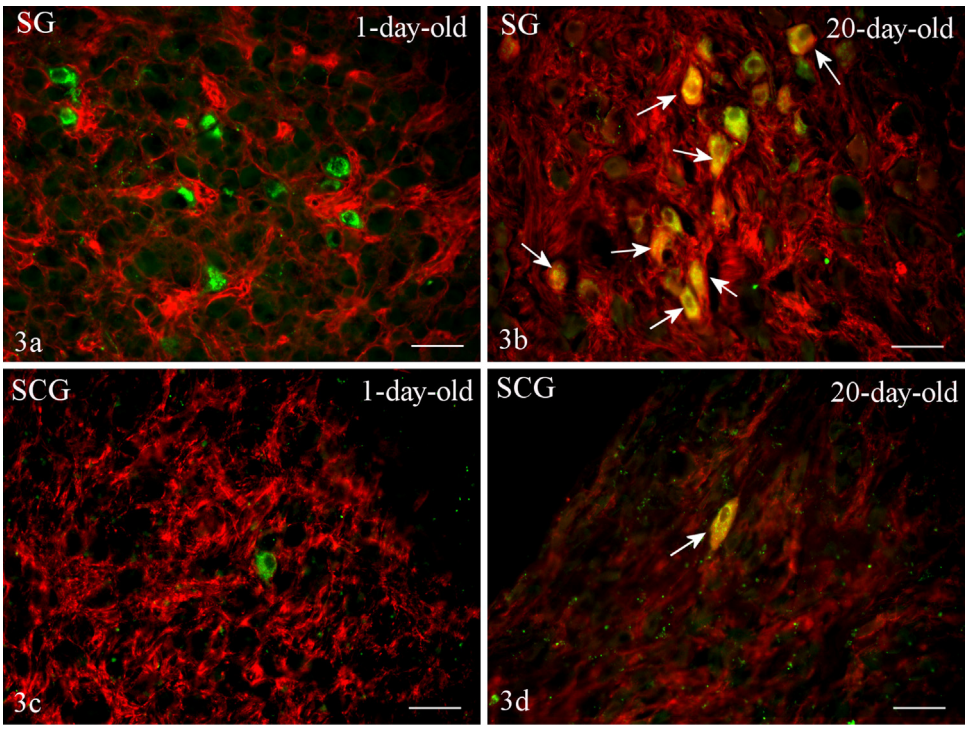

Fig. 3. Fluorescence micrographs of VIP-IR (green) and ChAT-IR (red) neurons in the SG (a and b), SCG (c and d) in newborn (a, c) and 30-day-old cats (b, d). There is no co-localization in (a) and (c). ChAT+/VIP+ IR neurons are indicated by arrows (b, d). Bar 50 μm. (For interpretation of the references to color in this figure legend, the reader is referred to the web version of this article.)

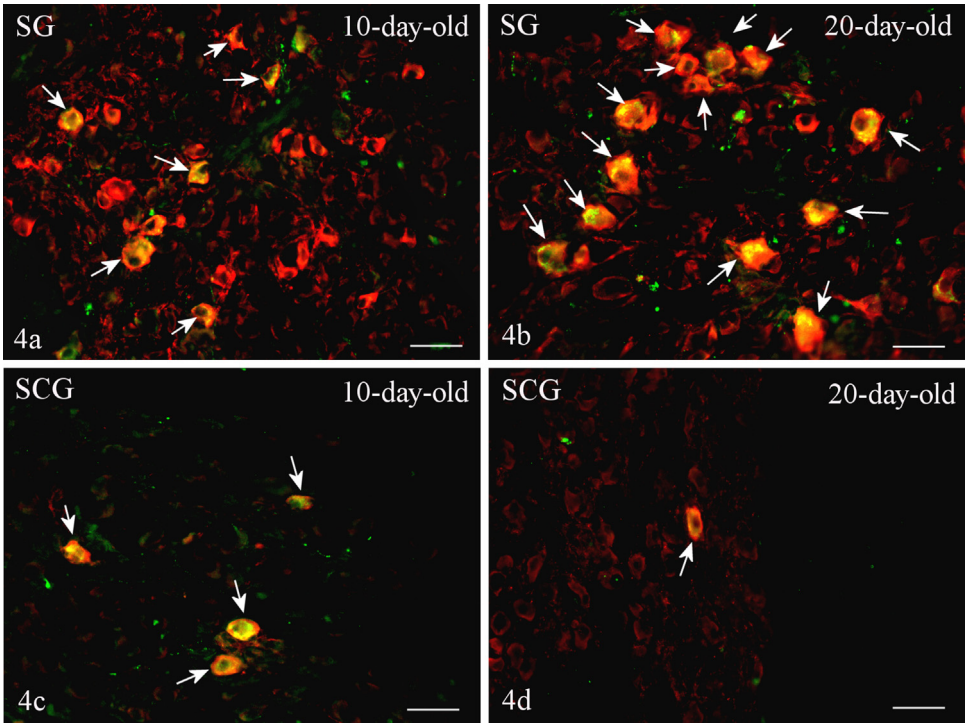

Fig. 4. Fluorescence micrographs of CGRP-IR (green) and nNOS-IR (red) neurons in the SG (a and b), SCG (c and d) in 10-day-old (a, c) and 20-day-old cats (b, d). CGRP+/nNOS+ IR neurons are indicated by arrows Bar 50 μm. (For interpretation of the references to color in this figure legend, the reader is referred to the web version of this article.)

are present from the moment of birth., The results of the present study show that VIP-IR and nNOS-IR neurons were TH-negative in newborn and older kittens, whereas previous data from our group as well as from others indicate that the vast majority of VIP-IR and ChAT-IR cells in the sympathetic ganglia of newborn rodents are characterized by the expression of both adrenergic and cholinergic traits and that they also express TH IR (Landis and Keefe, 1983; Leblanc and Landis, 1986; Masliukov et al., 2006; Cane and Anderson, 2009). Furthermore, their number was substantially lower in 10-day-old and older animals (Leblanc and Landis, 1986; Schäfer et al., 1997; Guidry and Landis, 1998; Masliukov et al., 2006).

In newborn kittens, non-catecholaminergic sympathetic ganglionic neurons were represented by VIP-IR and (or) nNOS-IR neurons. Marked levels of CGRP or ChAT IR in sympathetic neurons appeared after 10 days of life.

Previous experiments in adult cats with tract tracing have shown that clustered cells with strong VIP-IR but with no CGRP-IR are muscle vasodilator neurons. The scattered nNOS-IR neurons colocalizing CGRP-IR with weak VIP immunoreactivity are sudomotor neurons (Anderson et al., 1995). Possibly, in newborn kittens, clustered vasodilatator neurons express only VIP and a small number of presumptive sudomotor neurons are initially only nNOS-IR. The number of sudomotor neurons increased after birth and nNOS appeared earlier than VIP in this population of non-catecholaminergic cells. CGRP and VIP appeared in sudomotor ganglionic neurons, and ChAT in sudomotor and vasodilatator sympathetic neurons in 10-day-old kittens and their expression was more pronounced after 20 days of life.

Cross-sectional areas of sympathetic neurons increased in postnatal development. (Masliukov, 2001). VIP-IR and nNOS-IR neurons were larger in size compared to catecholaminergic TH-IR neurons from the moment of birth. In rodents, cholinergic ChAT-IR and VIP-IR neurons were also larger in size than TH-IR cells (Anderson et al., 2006; Masliukov et al., 2006).

VIP and NOS expression are regulated differently in different populations of sympathetic neurons. In rodents, the development of VIP expression differs substantially between the SG and SCG. No VIP IR was detected in the embryonic or neonatal SCG, whereas a large number of VIP-IR neurons were found in the SG. Early VIP expression is not related to the innervation of peripheral targets, and in the SG, the percentage of VIP-positive cells declined from 15% at ED 16.5 to 3.5% at birth, when adult proportions are established (Tyrrell and Landis, 1994; Ernsberger and Rohrer, 1999).

Previous data by our group have revealed that the changes in the number of NADPH-d-positive cells during development occur differently in the various sympathetic ganglia, which is now further substantiated by our current results about the development of nNOS-IR neurons. The proportion of NADPH-d-positive and nNOS-IR cells in the SG increased in first 20 days of life, whereas those in the CG and SCG did not change in number during development (Masliukov et al., 2003; Emanuilov et al., 2008).

In newborn kittens, contacts with target organs have already been established. Nevertheless, the number of connections of SG neurons with vessels of neck and forearm muscles increased in the first 20 days of development (Masliukov, 2000). Our current results show that this increase is accompanied by an increase in

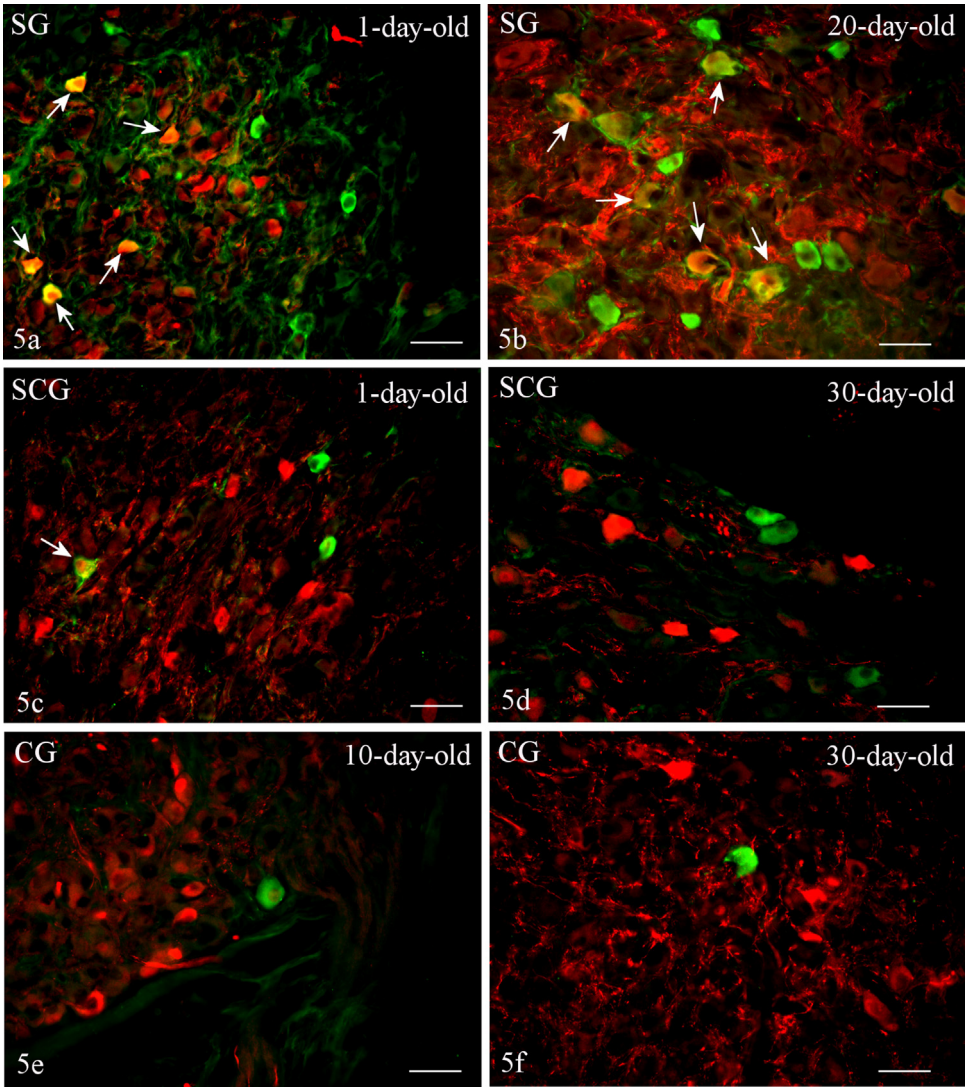

Fig. 5. Fluorescence micrographs of nNOS-IR (green) and CB-IR (red) neurons in the SG (a and b), SCG (c and d) and CG (e and f) in 1-day-old (a, c), 10-day-old (e), 20-day-old (b) and 30-day-old cats (d, f). nNOS+/CB+ IR neurons are indicated by arrows. Bar 50 μm. (For interpretation of the references to color in this figure legend, the reader is referred to the web version of this article.)

the number of nNOS-IR neurons, the majority of which surprisingly became sudomotor neurons. The number of presumptive vasodilatator clustered VIP-IR neurons did not change significantly throughout development. However, additional nNOS-IR neurons may be involved in vasodilatation, which accompanies and supports sweat secretion. In cats, collateral branches of sudomotor neurons innervate cutaneous blood vessels, where they release vasodilator transmitters including nitric oxide, VIP and CGRP (Anderson et al., 1995).

In chick sympathetic ganglia, the expression of VIP but not ChAT in sympathetic neurons depends on cytokines signaling through heterodimeric gp130/LIFRß receptors (Geissen et al., 1998; Duong et al., 2002). Cytokines include oncostatin M, cardiotrophin-like cytokine and neuropoietin/cardiotrophin 2 signalling via binding to receptor complexes (Heinrich et al., 2003). Cytokine binding results in the activation of the associated JAK tyrosine kinases and subsequent phosphorylation of both the receptor subunits and downstream signaling proteins (Apostolova and Dechant, 2009). Unlike in chicks, in mouse sympathetic stellate ganglia gp130 signaling is essential for the postnatal target-dependent expression of both VIP and ChAT (Stanke et al., 2006).

Both phenotypes (cholinergic and noradrenergic) are simultaneously induced by BMPs and transiently co-expressed at early developmental stages (Apostolova and Dechant, 2009). It has been reported that transcription factor *Phox2b* was required for the early cholinergic differentiation at E11.5 (Huber and Ernsberger, 2006). In mouse sympathetic ganglia, two stages in the development of cholinergic neurons were observed: (i) an embryonic stage, in which Ret the signal-transducing component of the receptor complex for glial cell line-derived neurotrophic factor (GDNF) and transcription factor *Tlx3* family ligands, plays a role; and (ii) a postnatal stage, which depends on target-derived neurokines (Burau et al., 2004; Stanke et al., 2006; Ernsberger, 2008). The transcription factor Tlx3 controls the cholinergic neuronal development and is required for the high-level expression of *Ret*. Expression of VIP requires *Tlx3* but not *Ret* at the early embryonic stage (E12.5), suggesting that *Tlx3* may be required for the initiation of VIP expression, whereas *Ret* is only needed for the maintenance of VIP expression. On the other hand, *Tlx3* and *Ret* are both required for VAChT expression at the late (E18.5 or newborn mice) but not the early (E12.5 or E13) embryonic stage (Burau et al., 2004; Huang et al., 2013).

VIP may act as a trophic factor for sympathetic neurons. This suggestion is supported by the observation that VIP was found to rescue a small population (10%) of post-mitotic sympathetic neurons derived from the neonatal SCG after withdrawal of nerve growth factor (Klimaschewski, 1997). Axotomy induces or increases the number of neurons expressing VIP and/or NOS in sympathetic ganglia in rodents but not in pigs (Shadiack et al., 2001; Wojtkiewicz et al., 2013).

Unfortunately, data on the factors that influence nNOS expression during development are scarce. However, NO is an important modulator of proliferation in many types of normal and tumor cells (Villalobo, 2006; Peña-Altamira et al., 2010). Some data point to a transient overexpression of NOS in both the neuropil and specific neuronal populations of the developing cerebral cortex (Judas et al., 1999). In embyogenesis, NO plays a role in axon pathfinding (Berman and Morris, 2011). However, the exact role of NO in the development of sympathetic neurons still needs to be established.

In cats, CB is found in a number of presumptive sympathetic sudomotor neurons but not in muscle vasodilatator neurons in the initial period of postnatal life, which may be linked to changes in neurotransmitter properties observed in this population of neurons in the SG, especially with the appearance of nNOS and VIP in these cells because late expression of CGRP and ChAT is observed in all studied sympathetic ganglia, in sudomotor and vasodilatator neurons. In mature neurons, calcium-binding proteins are involved in numerous functions, including cell signaling, calcium uptake and transport, cell motility and intracellular calcium buffering. CB may protect neurons against large fluctuations in free intracellular Ca^{2+} and may prevent cell death (Andressen et al., 1993; Schwaller, 2012). Possibly, CB is necessary to establish new synaptic contacts between axons of principal ganglionic neurons and target organs, preganglionic fibers and principal ganglionic neurons. Among the factors that regulate synaptic development and plasticity, calcium signaling has received particular attention because its dynamics are specifically controlled in space and time (Siechen et al., 2009; Heiman and Shaham, 2010). At each stage of synaptic development, calcium signaling is spatially confined to individual synapses by specialized calcium-handling mechanisms involving calcium channels, buffers and transporters, as well as by structural compartments. (Michaelsen and Lohmann, 2010).

5. Conclusions

In summary, the present study provides further insight into the development of non-catecholaminergic sympathetic neurons in cats. In newborn animals, the majority of non-catecholaminergic neuron have one main neurotransmitter – VIP or NO. CGRP and ChAT appear after 10 days of life. The various sympathetic ganglia (SCG, SG and CG) each follow their own distinct pattern of development and co-localization of cholinergic markers. CB is found in a number of presumptive sympathetic sudomotor neurons but not in muscle vasodilatator neurons in the initial period of postnatal life. However, the mechanism of expression of VIP, NO, CGRP and ChAT as well as their relation with CB remain to be elucidated in cats. Further studies are required to identify target-dependent and independent pathways of their expression. The information provided in this study will also serve as a basis for future studies that investigate the mechanisms underlying the development of sympathetic neurons.

Acknowledgement

This work was supported by Russian Fund for Basic Research (RFBR), grant 13-04-00059.

References

Anderson, C.R., Bergner, A., Murphy, S.M., 2006. How many types of cholinergic sympathetic neuron are there in the rat stellate ganglion? Neuroscience 140, 567–576.
Anderson, C.R., McAllen, R.M., Edwards, S.L., 1995. Nitric oxide synthase and chemical coding in cat sympathetic postganghonic neurons. Neuroscience 68, 255–264.
Andressen, C., Blumcke, I., Celio, M.R., 1993. Calcium-binding proteins: selective markers of nerve cells. Cell Tissue Res. 271, 181–208.
Apostolova, G., Dechant, G., 2009. Development of neurotransmitter phenotypes in sympathetic neurons. Auton. Neurosci. 151, 30–38.
Asmus, S.E., Tian, H., Landis, S.C., 2001. Induction of cholinergic function in cultured sympathetic neurons by periosteal cells: cellular mechanisms. Dev. Biol. 235, 1–11.
Berman, S., Morris, A., 2011. Nitric oxide as a putative retinal axon pathfinding and target recognition cue in *Xenopus laevis*. Impulse (Columbia) 2010, 1–12.
Bolem, P., Fuxe, K., 1970. Adrenergic and cholinergic nerve terminals in skeletal muscle vessels. Acta Physiol. Scand. 78, 53–59.
Burau, K., Stenull, I., Huber, K., Misawa, H., Berse, B., Unsicker, K., Ernsberger, U., 2004. c-Ret regulates cholinergic properties in mouse sympathetic neurons: evidence from mutant mice. Eur. J. Neurosci. 20, 353–362.
Cane, K.N., Anderson, C.R., 2009. Generating diversity: mechanisms regulating the differentiation of autonomic neuron phenotypes. Auton. Neurosci. 151, 17–29.
Duong, C.V., Geissen, M., Rohrer, H., 2002. The developmental expression of vasoactive intestinal peptide (VIP) in cholinergic sympathetic neurons depends on cytokines signaling through LIFRbeta-containing receptors. Development 129, 1387–1396.
Emanuilov, A.I., Korzina, M.B., Archakova, L.I., Novakovskaya, S.A., Nozdrachev, A.D., Masliukov, P.M., 2008. Development of the NADPH-diaphorase-positive neurons in the sympathetic ganglia. Ann. Anat. 190, 516–524.

Ernsberger, U., 2008. The role of GDNF family ligand signalling in the differentiation of sympathetic and dorsal root ganglion neurons. Cell Tissue Res. 333, 353–371.
Ernsberger, U., Rohrer, H., 1999. Development of the cholinergic neurotransmitter phenotype in postganglionic sympathetic neurons. Cell Tissue Res. 297, 339–361.
Geissen, M., Heller, S., Pennica, D., Ernsberger, U., Rohrer, H., 1998. The specification of sympathetic neurotransmitter phenotype depends on gp130 cytokine receptor signaling. Development 125, 4791–4801.
Guidry, G., Landis, S.C., 1998. Target-dependent development of the vesicular acetylcholine transporter in rodent sweat gland innervation. Dev. Biol. 199, 175–184.
Heiman, M.G., Shaham, S., 2010. Twigs into branches: how a filopodium becomes a dendrite. Curr. Opin. Neurobiol. 20, 86–91.
Heinrich, P.C., Behrmann, I., Haan, S., Hermanns, H.M., Muller-Newen, G., Schaper, F., 2003. Principles of interleukin (IL)-6-type cytokine signalling and its regulation. Biochem. J. 374, 1–20.
Hope, B.T., Michael, G.J., Knigge, K.M., Vincent, S.R., 1991. Neuronal NADPH-diaphorase is a nitric oxide synthase. Proc. Natl. Acad. Sci. 88, 2811–2814.
Huber, K., Ernsberger, U., 2006. Cholinergic differentiation occurs early in mouse sympathetic neurons and requires Phox2b. Gene Expr. 13, 133–139.
Huang, T., Hu, J., Wang, B., Nie, Y., Geng, J., Cheng, L., 2013. Tlx3 controls cholinergic transmitter and peptide phenotypes in a subset of prenatal sympathetic neurons. J. Neurosci. 33, 10667–10675.
Järhult, J., Hellstrand, P., Sundler, F., 1980. Immunohistochemical localization and vascular effects of vasoactive intestinal polypeptide in skeletal muscle of the cat. Cell Tissue Res. 207, 55–64.
Judas, M., Sestan, N., Kostović, I., 1999. Nitrinergic neurons in the developing and adult human telencephalon: transient and permanent patterns of expression in comparison to other mammals. Microsc. Res. Tech. 45, 401–419.
Klimaschewski, L., 1997. VIP – a 'very important peptide' in the sympathetic nervous system? Anat Embryol. (Berl.) 196, 269–277.
Klimaschewski, L., Kummer, W., Heym, C., 1996. Localization: regulation and functions of neurotransmitters and neuromodulators in cervical sympathetic ganglia. Microsc. Res. Tech. 35, 44–68.
Landis, S.C., 1988. Neurotransmitter plasticity in sympathetic neurons and its regulation by environmental factors in vitro and in vivo. In: Björklund, A., Hökfelt, T., Owman, C. (Eds.), Handbook of Chemical Neuroanatomy. The Peripheral Nervous System. Elsevier, Amsterdam – New York – Oxford, pp. 65–115.
Landis, S.C., Keefe, D., 1983. Evidence for neurotransmitter plasticity in vivo: developmental changes in properties of cholinergic sympathetic neurons. Dev. Biol. 98, 349–372.
Leblanc, G.G., Landis, S.C., 1986. Development of choline acetyltransferase (CAT) in the sympathetic innervation of rat sweat glands. J. Neurosci. 6, 260–265.
Lindh, B., Lundberg, J.M., Hökfelt, T., 1989. VIP/PHI-, NPY- galanin-, CGRP- and substance P-immunoreactive neuronal subpopulations in cat autonomic and sensory ganglia and their projections. Cell Tissue Res. 256, 259–273.
Masliukov, P.M., 2000. Connections of the cat stellate ganglion with target organs during postnatal ontogenesis. Ross. Fiziol. Zh. Im I. M. Sechenova 86, 703–710.
Masliukov, P.M., 2001. Sympathetic neurons of the cat stellate ganglion in postnatal ontogenesis: morphometric analysis. Auton. Neurosci. 89, 48–53.
Masliukov, P.M., Nozdrachev, A.D., Timmermans, J.P., 2006. The age specifics of the neurotransmitter composition of the stellate ganglion neurons. Ross. Fiziol. Zh. Im I. M. Sechenova 92, 214–220.
Masliukov, P.M., Shilkin, V.V., Nozdrachev, A.D., Timmermans, J.-P., 2003. Histochemical features of neurons in the cat stellate ganglion during postnatal ontogenesis. Auton. Neurosci. 106, 84–90.
Masliukov, P.M., Korobkin, A.A., Nozdrachev, A.D., Timmermans, J.P., 2012. Calbindin-D28k immunoreactivity in sympathetic ganglionic neurons during development. Auton. Neurosci. 167, 27–33.
Masliukov, P.M., Emanuilov, A.I., Madalieva, L.V., Moiseev, K.Y., Bulibin, A.V., Korzina, M.B., Porseva, V.V., Korobkin, A.A., Smirnova, V.P., 2014. Development of nNOS-positive neurons in the rat sensory and sympathetic ganglia. Neuroscience 256, 271–281.
Michaelsen, K., Lohmann, C., 2010. Calcium dynamics at developing synapses: mechanisms and functions. Eur. J. Neurosci. 32, 218–223.
Peña-Altamira, E., Petazzi, P., Contestabile, A., 2010. Nitric oxide control of proliferation in nerve cells and in tumor cells of nervous origin. Curr. Pharm. Des. 16, 440–450.
Santer, R.M., Symons, D., 1993. Distribution of NADPH-diaphorase activity in rat paravertebral: prevertebral and pelvic sympathetic ganglia. Cell Tissue Res. 271, 115–121.
Schäfer, M.K.H., Schuetz, B., Weihe, E., Eiden, L.E., 1997. Target-independent cholinergic differentiation in the rat sympathetic nervous system. Proc. Natl. Acad. Sci. U.S.A. 94, 4149–4154.
Schäfer, M.K.H., Eiden, L.E., Weihe, E., 1998. Cholinergic neurons and terminal fields revealed by immunohistochemistry for the vesicular acetylcholine transporter. II. The peripheral nervous system. Neuroscience 84, 361–376.
Schütz, B., von Engelhardt, J., Gördes, M., Schäfer, M.K., Eiden, L.E., Monyer, H., Weihe, E., 2008. Sweat gland innervation is pioneered by sympathetic neurons expressing a cholinergic/noradrenergic co-phenotype in the mouse. Neuroscience 156, 310–318.
Schwaller, B., 2012. The use of transgenic mouse models to reveal the functions of Ca^{2+} buffer proteins in excitable cells. Biochim. Biophys. Acta 1820, 1294–1303.
Shadiack, A.M., Sun, Y., Zigmond, R.E., 2001. Nerve growth factor antiserum induces axotomy-like changes in neuropeptide expression in intact sympathetic and sensory neurons. J. Neurosci. 21, 363–371.
Siechen, S., Yang, S., Chiba, A., Saif, T., 2009. Mechanical tension contributes to clustering of neurotransmitter vesicles at presynaptic terminals. Proc. Natl. Acad. Sci. U.S.A. 106 (2009), 12611–12616.
Spessert, R., Wohlgemuth, C., Reuss, S., Layes, E., 1994. NADPH-diaphorase activity of nitric oxide synthase in the olfactory bulb: co-factor specifity and characterization regarding the interrelation to NO formation. J. Histochem. Cytochem. 42, 569–575.
Stanke, M., Duong, C.V., Pape, M., Geissen, M., Burbach, G., Deller, T., Gascan, H., Otto, C., Parlato, R., Schutz, G., Rohrer, H., 2006. Target-dependent specification of the neurotransmitter phenotype: cholinergic differentiation of sympathetic neurons is mediated in vivo by gp 130 signaling. Development 133, 141–150.
Tyrrell, S., Landis, S.C., 1994. The appearance of NPY and VIP in sympathetic neuroblasts and subsequent alterations in their expression. J. Neurosci. 14, 4529–4547.
Villalobo, A., 2006. Nitric oxide and cell proliferation. FEBS J. 273, 2329–2344.
Weihe, E., Tao-Cheng, J.H., Schäfer, M.K.H., Erickson, J.D., Eiden, L.E., 1996. Visualization of the vesicular acetylcholine transporter in cholinergic nerve terminals and its targeting to a specific population of small synaptic vesicles. Proc. Natl. Acad. Sci. U.S.A. 93, 3547–3552.
Wojtkiewicz, J., Równiak, M., Crayton, R., Gonkowski, S., Robak, A., Zalecki, M., Majewski, M., Klimaschewski, L., 2013. Axotomy-induced changes in the chemical coding pattern of colon projecting calbindin-positive neurons in the inferior mesenteric ganglia of the pig. J. Mol. Neurosci. 51 (1), 99–108.